Transactions of the VŠB – Technical University of Ostrava, Mechanical Series
No. 2, 2013, vol. LIX
article No. 1951

Michał BARCIKOWSKI[*], Wacław KRÓLIKOWSKI[**]

CHARACTERISTICS OF IMPACT DAMAGE AND POST-IMPACT STRENGTH IN GLASS-FIBRE-REINFORCED PLASTICS WITH DIFFERENT REINFORCEMENT ARCHITECTURE

CHARAKTERISTIKY IMPAKTNÍHO POŠKOZENÍ A PONÁRAZOVÉ PEVNOSTI VLÁKNOVÝCH PLASTOVÝCH KOMPOZITŮ S RŮZNOU ARCHITEKTUROU SKELNÉ VÝZTUŽE

Abstract

Fiber-reinforced plastics (FRP) are nowadays used commonly for constructions subjected to impacts of different energies and velocities; therefore, the problem of impact resistance is crucial. This paper presents the results of high-velocity impact tests and post-impact evaluation of damage in glass-fiber-reinforced plastics, depending on the architecture of reinforcing material (different woven fabrics, mat). Composites reinforced with continuous-filament mat, woven roving, roving fabric and twisted-yarn fabric were prepared and subjected to intermediate- and high-velocity impact. After the ballistic impact, damage extent and residual strength, as well as water leakage through the composites, were evaluated. The damage was also investigated under a microscope. The damage extent was confirmed to be linearly dependent on impact energy. The addition of rubber was found to decrease damage extent and increase post-impact residual strength, as well as decrease water leakage rate.

Abstrakt

Plasty vyztužené vlákny (FRP) jsou v současné době hojně používány pro konstrukce vystavené nárazům o různé energii a rychlosti. Z tohoto důvodu je řešení problematiky odolnosti proti nárazu klíčové. Tento článek prezentuje výsledky vysokorychlostních nárazových zkoušek v případě plastů vyztužených skelnými vlákny v závislosti na architektuře matrice (různé druhy tkanin). Kompozity vyztužené spojitými vlákny s různým zpracováním byly posléze podrobeny nárazovým zkouškám s různou rychlostí indentoru. Po nárazu byl zkoumán rozsah poškození, reziduální pevnost a také intenzita úniku vody skrz poškozenou oblast, která byla dodatkově analyzována s využitím mikroskopu. Zkoušky potvrdily lineární závislost mezi rozsahem poškození a nárazovou energií. Přidáním kaučuku do základní matrice došlo ke zvýšení zbytkové pevnosti kompozitu včetně snížení intenzity úniku vody skrz poškozený kompozit.

Keywords

Composite materials, glass-fibre-reinforced plastics, impact tests, multiple impact, residual strength, post-impact strength, reinforcement architecture, delamination, damage extent, fracture

[*] dr inż., Institute of Materials Science and Applied Mechanics, Faculty of Mechanical Engineering, Wrocław University of Technology, Smoluchowskiego 25, Wrocław, tel. (+48) 71 320 4783, e-mail: michal.barcikowski@pwr.wroc.pl

[**] prof. dr inż., Polymer Institute, Faculty of Chemical Technology and Engineering, West Pomeranian University of Technology, Pulaskiego 10, Szczecin, tel. (+48) 91 449 4247, e-mail: ip@zut.edu.pl

1 INTRODUCTION

Fibre-reinforced plastics (FRP) are increasingly common as a construction material, where they are subjected to a wide range of loading conditions, among them impact loading [1]. There is a high probability of laminated elements being struck by objects of varying mass, shape and speed. The very thing that provides the ease of tailoring FRP properties – the multitude of structural components and the links between them – causes easy dissipation of impact energy and often irreversible damage to the material itself. Multiple phases and the bonding between them allow relatively easy dissipation of impact energy while at the same time lead to irreversible damage. The energy absorption and damage resistance are two conflicting qualities – the main mode of energy absorption is the damage itself [2].

Impact events may differ in velocity, energy and mass of impactor, mass of the target and geometry of a setup. The velocity of impact is of foremost importance – it may be used as a criterion for impact classification after Abrate [3]. The velocity affects, among else, the fracture mechanics of composite matrix material [4].

Low-velocity impacts are the most prevalent and most commonly tested of impact events. They are characterized by velocity of below 10 m/s. The duration of impact is much longer than the time needed for an elastic wave to travel to the objects edge [3, 5-7]. This type of impact is also labeled as quasi-static due to similar stress distribution [7-8]. Support conditions are the deciding factor in this instance [5, 8]. Such impact is most commonly associated with unintentional collisions and falls from heights. The well-known Charpy impact tests fall in this range.

High-velocity impacts, called also ballistic impacts, are characterized by impact velocity in the range of 100-1000 m/s. The duration of impact is comparable to the time of elastic waves propagation in the direction perpendicular to the surface [3, 7]. Damage is confined to the vicinity of impact because the elastic waves didn't propagate further. The main cause of damage is local excess over material strength on the wave front [3, 5-7, 9]. This type of impacts is most commonly associated with gunfire, shell fragments and collisions of aircraft with various objects.

During an impact event, the impactor dissipates its kinetic energy. In FRP targets, there may occur some or all of the following energy-dissipation mechanisms: transformation into the kinetic energy of targets moving part, fiber deformation, tensile fiber failure, fiber shear, delamination and matrix cracking, heat release, impactor-target friction, and the deformation of the impactor itself [5, 9-14]. Of these, the most prominent are target kinetic energy and fibre failure [10-13] while delamination and matrix cracking are the primary cause of post-impact strength reduction [5,12,16-18]. Since matrix cracking and delamination occur together – in fact, the former initiates the latter – no attempt to discern between the two damage types is feasible [12]. Fibre breakage and misorientation is expected after sufficiently heavy impacts [18].

Evaluation of the damage severity in FRP after the impact event is crucial. Impact damage in laminates usually consists of an impactor footprint and a surrounding field of delamination together with co-occurring matrix cracking. The extent of delamination (and assumed matrix cracking) damage is usually much larger than the impact footprint itself. The higher the impact energy is, the larger the delaminated region area. The extent of a region delaminated as a result of impact is usually evaluated using one of several non-destructive investigation (NDI) methods: optical image analysis, air or water-coupled ultrasonic defectoscopy, roentgenography and impulsive-thermographic method. The area of delamination is deemed to be proportional to the impact energy for non-penetrating impacts [14-15].

The salient question is how the impact and impact-induced damage affect the residual strength of composite panel. Composites residual strength investigation is quite common after low-velocity impacts, but rather uncommon after ballistic impacts. Quasi-static tests of specimens subjected to impact are common. Depending on working conditions envisioned for the material, specimens may be tested in tension, compression, flexion or indentation. Flexural tests are easier to conduct than compressive, don't need unique equipment and aren't laden with uncertainties associated with

compressive tests [17]. Besides quasi-static post-impact tests, follow-on impact tests are also conducted. Post-impact tests may also include fatigue tests.

The objective of this work was to investigate the effect of reinforcement architecture in glass/polyester composites on the extent and characteristics of the field of damage resulting from high-velocity impact of known energy, as well as on the residual strength of damaged composite material.

2 MATERIALS AND METHODS

Composite plates, of 520x520 mm dimensions and 4 mm thick, were produced with resin transfer moulding (RTM) technology. GEPO type RTM mini aggregate was used. 1.5 phr MEKP were used as an initiator, and 0.6 ml/kg of 10% cobalt accelerator was added. The infusion of reinforcement by the resin was conducted through central inlet, and the air and excess of resin were evacuated through four outlets in corners of the stiff two-part mold. Resin curing was conducted at room temperature.

Polimal 109-32K (Z.Ch. Organika Sarzyna, Poland) unsaturated polyester resin was used for the matrix. The reinforcement consisted of E-type glass fibre in the form of continuous-filament mat (CFM), woven roving (6WR and 10WR – differing by fibre volume fraction), roving fabric (RF) and twisted-yarn fabric (TYF).

Specimens (100x100x4 mm) cut from moulded plates were subjected to ballistic impact using a gas gun. The specimens were freely supported in corners, and the site of impact was in the center of the specimen. Spherical steel impactor had a mass of 2.0 g and diameter of 8 mm. The impact energy was varied between 7 and 17 J (90-130 m/s). This means the impacts fell in sub-ballistic and ballistic regimes. The impactor muzzle velocity is measured by an attached ballistic chronograph. The difference between the muzzle and incident velocity is deemed negligible due to the short distance between the barrel muzzle and the specimen. The impactor velocity was varied by varying the compressed air pressure. Varying energy was used to establish the shape of damage extent dependence on impact energy. This test were conducted using specially built pneumatic test assembly shown in fig. 1.

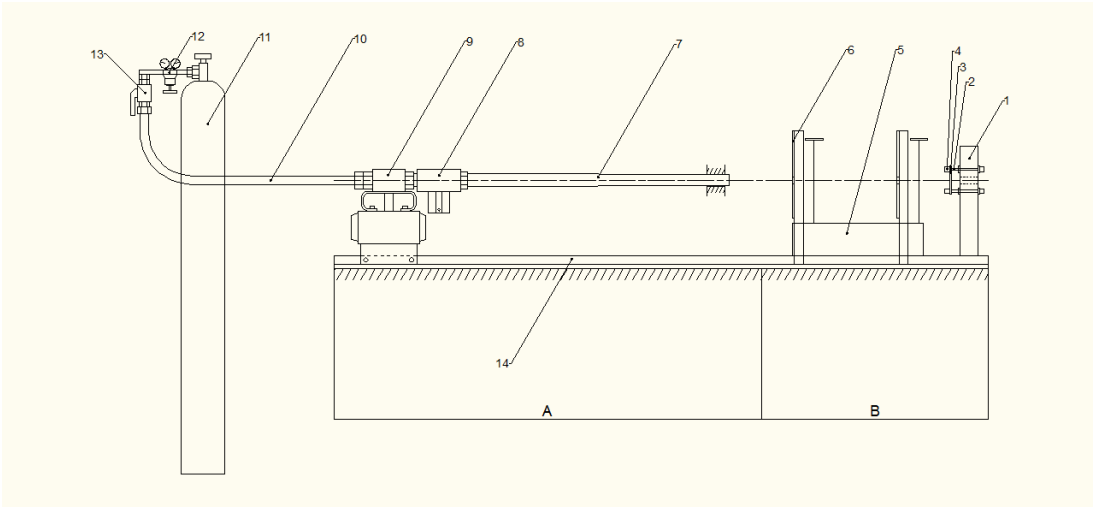

Fig. 1 Schematics of the ballistic assembly: A – propelling part, B – measurement part, 1 – base plate, 2 – specimen support, 3 – specimen, 4 – magnet, 5 – ballistic chronograph, 6 – anti-blast screen, 7 – barrel, 8 – receiver, 9 – electropneumatic valve, 10 – compressed-air duct, 11 – compressed-air tank, 12 – gas reductor, 13 – shut-off valve, 14 – montage rail

The ballistic damage to the plates was evaluated through following methods:

- measurement of damage area as visible in transmitted light;
- post-impact mechanical tests of damaged plate and calculation of the residual strength of damage region alone;
- evaluation of damage escalation after subsequent impacts into damage plate;
- assessment of the leakage of water through the damaged plate under given water column;
- microscopic examination of damage in microsections of the plates.

The extent of delamination (co-occurring with matrix cracking) was evaluated by means of a digital image analysis – the samples were photographed in transmitted light using a digital camera. Obtained images were processed using Scion Image software to measure the contrasting delaminated area.

In order to evaluate the post-impact residual strength of the composite, 12 specimens of each material were subjected to impact at mean energy of 11.5 J. These specimens were then subjected to a 3-point flexural test (fig. 2) and compared to virgin samples. Three-point quasi-static bending was conducted on the Instron 4206 universal testing machine with computerized data acquisition. Samples were square plates 100x100x4 mm. The testing method was based on ISO 178:1996 standard but modified to suit specific experimental needs. The procedure followed practice described previously in [19-20]. Samples without prior impact were tested for comparison. The results are presented here as a post-impact strength of the material from the damaged region alone, calculated according to previously developed method [19-20]. The post-impact strength is presented as a percentage, where 100% correspond to the strength of undamaged material.

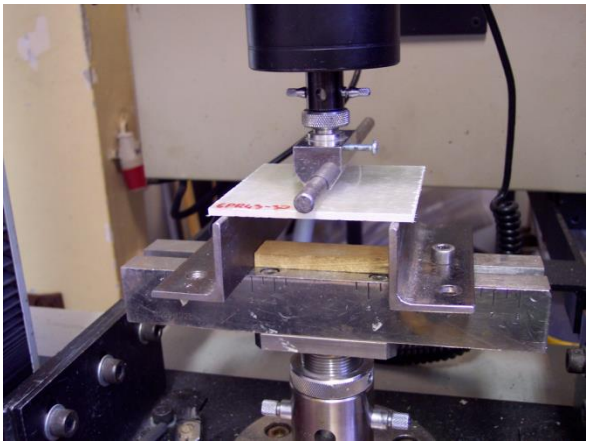

Fig. 2 Sample undergoing three-point quasi-static flexural test

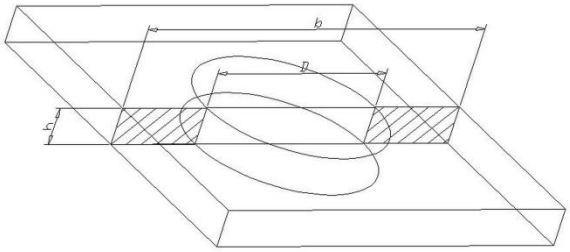

Fig. 3 Sample with cut-out circular hole. Remaining effective cross-section highlighted

We may consider what effect the complete elimination of the damaged field would have on the load-at-break of the sample. Since the impact damage has a roughly-circular shape in the plane of the plate, we will use the surface area of a circle for further consideration. If we imagine (Figure 3) cutting a circular hole with a surface area (S) equal to the surface area of the damaged field (S_D), we will lose from the sample's total cross-sectional area (A_{tot}) a rectangle with a length equal to the circle diameter (D) and width of the sample thickness (h). Since A_{tot} is a rectangle with the length of b and width h, the effective cross-sectional area would be expressed as in Equation (1):

$$A_{eff} = A_{tot} - D * h = (b - D) * h, \tag{1}$$

where:

A_{eff} – effective cross-section $\left[mm^2\right]$,

A_{tot} – total cross-section $\left[mm^2\right]$,

D – diameter of the cut-out/equivalent diameter of the damaged area $\left[mm\right]$,

h – specimen thickness $\left[mm\right]$,

b – specimen breadth $\left[mm\right]$.

This would lead to the ratio expressed in Equation 2:

$$\frac{A_{eff}}{A_{tot}} = \frac{D}{b}, \tag{2}$$

The load-at-break, which the sample is able to bear, is directly proportional to A_{eff}; thus, the critical load of a sample with a cut-out hole should be equal to an undamaged sample critical load multiplied by a D/b ratio. This logic is supported by previous works.

This would be the most severe form of damage - removing the load-bearing abilities of the entire damaged field. The least severe would be of course a load-bearing ability equal to that of the undamaged field in the sample. The real samples with impact damage should fall somewhere in-between. For each of them, we may assume a maximal load-at-break (F_{max}), which it could bear if undamaged. We can also calculate (from the damaged area) a theoretical minimum load-at-break (F_{min}) that it could bear if the entire damaged area were removed. By taking this minimal load-at-break and subtracting it from the actual tested load-at-break (F_{act}) of the sample, we may evaluate the actual residual load-bearing ability (F_{res}) of the damaged area. We may present it as a value (F_{res}, expressed in Equation (3)) or as a percentage ($F_{\%res}$, expressed in Equation (4)) assuming a worst-case scenario (damaged area entirely removed) load-at-break as 0% and best-case scenario (no real damage) load-at-break as 100%.

$$F_{res} = F_{act} - F_{\min}, \tag{3}$$

where:

F_{res} – residual load-at-break $\left[N\right]$,

F_{act} – actual load-at-break of the specimen $\left[N\right]$,

F_{min} – theoretical minimum load-at-break $\left[N\right]$.

$$F_{\%res} = \frac{F_{act} - F_{\min}}{F_{\max} - F_{\min}} * 100\%, \tag{4}$$

where:

$F_{\%res}$ – percentage residual load-at-break $[\%]$,

F_{max} – maximum load-at-break of the specimen (undamaged) $[N]$.

Percentage residual strength is equal to the percentage load-at-break (Equation (5)):

$$R_{\%res} = \frac{F_{res}}{D * h} = F_{\%res}, \tag{5}$$

where:

$R_{\%res}$ – percentage residual strength $[\%]$.

A multiple impact test was also performed on selected materials, in which a sample was repeatedly impacted at the point of original impact, with constant energy equaling to 16 Joules, as many times as was required to achieve complete perforation of the target sample.

An interesting evaluation of the damage severity is given by testing water leakage through the impact-damaged composite plate, following the method described in [21-22]. Water leakage was tested by placing the damaged sample under 500 mm column of water. The volume of water leaking through the material in given time was measured.

Selected samples of each material damaged by the impact were sectioned using a diamond saw diametrically through the field of damage. The resulting surface was then prepared through grinding and polishing, and investigated using a 3D scanning laser microscope Keyence VK-9700 series under 100x magnification. For each sample, several images were made, encompassing the whole area of the section. The individual images were then assembled into one large image.

3 RESULTS AND DISCUSSION

Fig. 4 presents the results of damage extent in composites after impacts of various energy. The area of damage is linearly dependent on impact energy, as would be expected. Composites reinforced with continuous-filament mat (CFM), roving fabric (RF) and twisted-yarn fabric (TYF) perform remarkably similarly to each other. The outliers are two composites reinforced with woven rovings (6WR and 10WR) – it is surprising because woven rovings are very similar in architecture to the other woven fabrics – RF and TYF, differing mainly in areal weight of the fabric and tow weight of individual fiber strands, as well as exact manufacturing technology (woven using rapier looms instead of flying-shuttle looms). The woven rovings exhibit, however, structure that is looser and permit larger degree of freedom of movement for individual fiber strands. This may have a role in distributing the impact energy over a larger area. Reinforcement architectures that constrain the freedom of movement of the individual strand may lead to a greater confinement of the damage, which is a known and sometimes encouraged behavior [23-26].

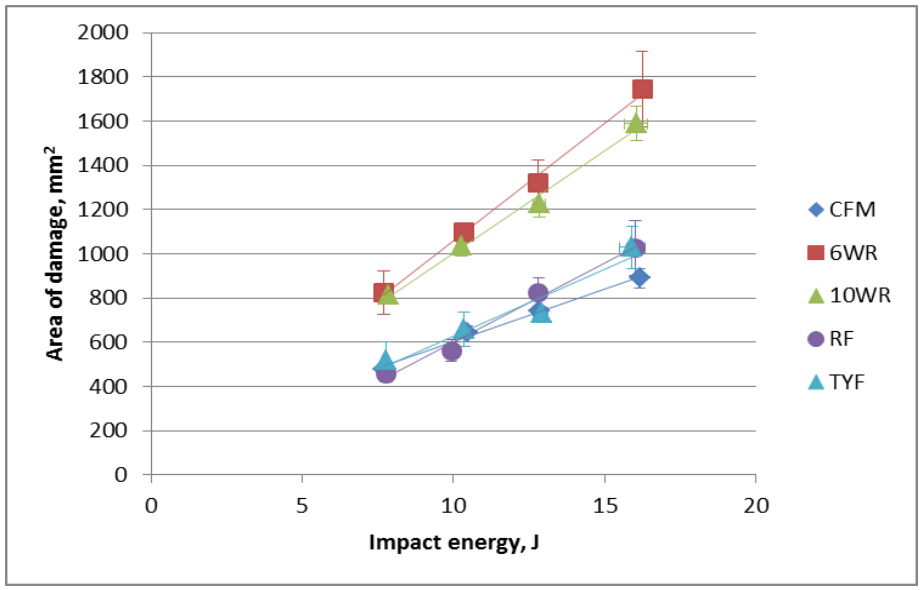

Fig. 4 Damage extent in composites after impacts of various energy

Fig. 5 presents the results of residual strength of the damaged region alone, calculated according to previously described method. As may be seen, different architectures of the reinforcement lead to a wide range of residual strength, from around 50% to around 90% of the strength of the undamaged material. The residual strength of the damaged area of the composite 10WR even achieved, together with the uncertainty bracket, level comparable to the strength of undamaged material. The best residual strength is exhibited by composites reinforced with woven roving. Higher reinforcement content led to higher residual strength. The lowest residual strength, together with the highest uncertainty level, is exhibited by the CFM-reinforced composite. The dispersion of the results is generally high. It may be a result of added dispersions of individual elements: undamaged material properties, impact energy, material response to impact of given energy.

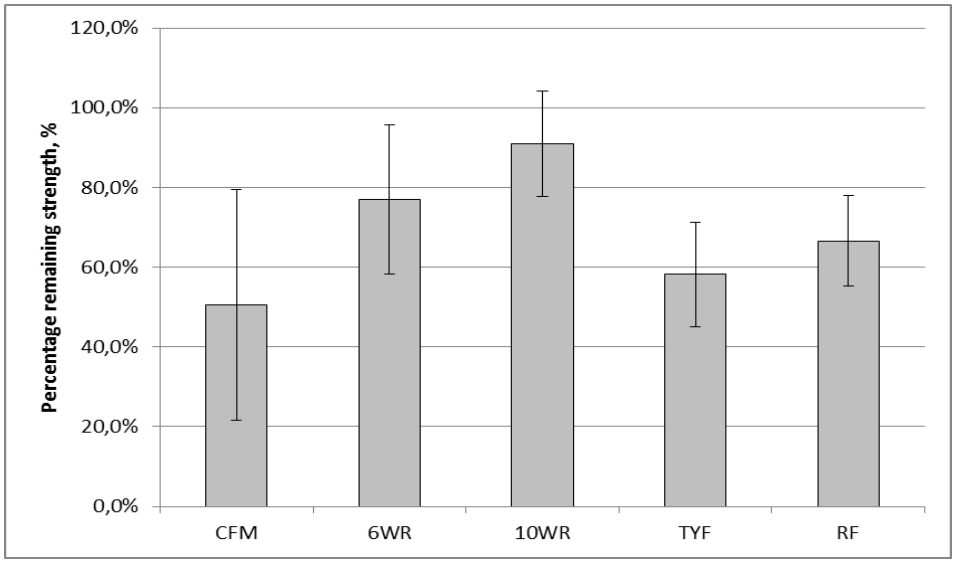

Fig. 5 Residual strength of the damaged region of the composites

Fig. 6 presents the results of the multiple-impact test of three composite materials: CFM, 10RT and TYF. After consecutive impacts, the extent of damage region increases. The last point of each of the lines on the graph corresponds with perforation of the plate. The growth of damage area is directly proportional to the number of impacts. Samples reinforced with woven fabrics required higher number of impacts than CFM-reinforced one. Their areas of damage increased with following impacts faster, however. In every material, every impact led to an equal increase in an area of damage, up to the penetrating impact, which usually caused only minimum, if at all, increase. That means that the energy of non-penetrating impact is absorbed each time by the same surface area of the composite.

a)

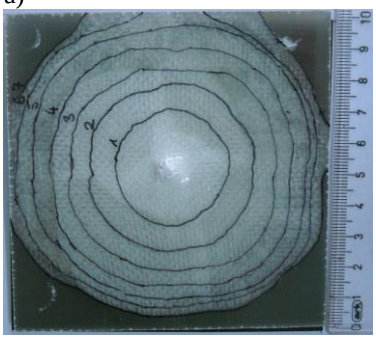

b)

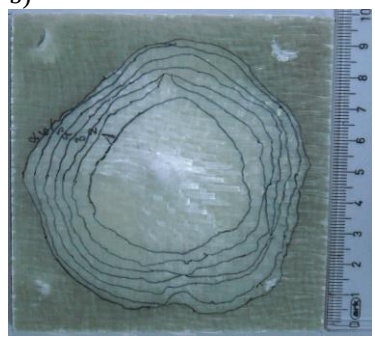

c)

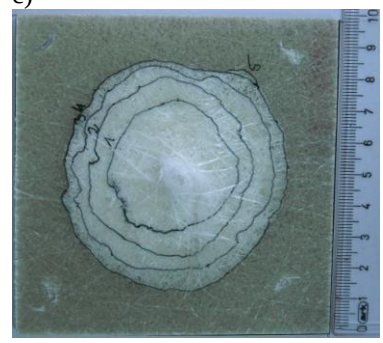

d)

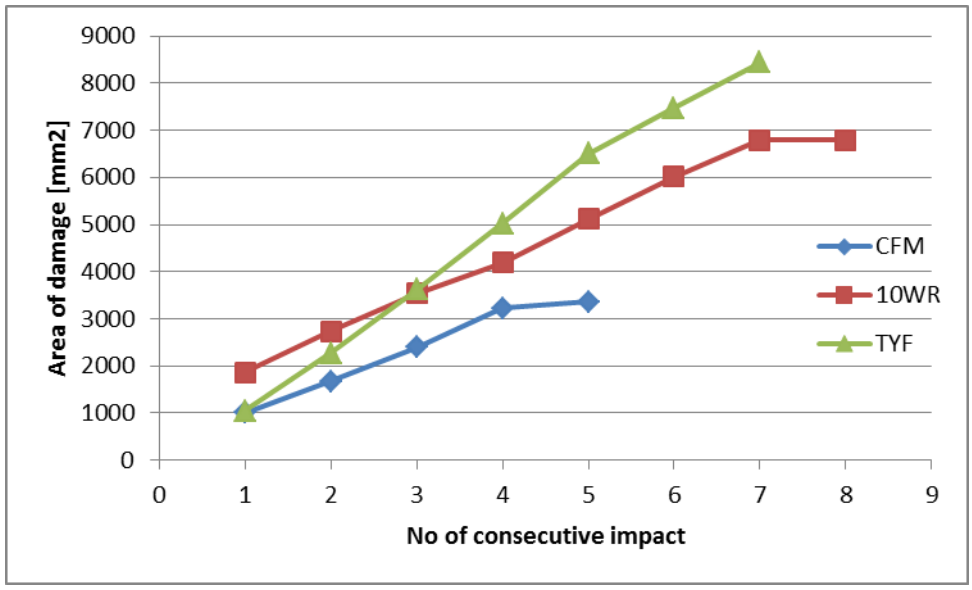

Fig. 6 Results of the multiple-impact test of three composite materials: a) photograph of a damage extent in TYF, b) photograph of a damage extent in 10WR, c) photograph of a damage extent in CFM, d) damage extent after consecutive impacts graph

Table 1 presents the above-mentioned results, as well as the results of the leakage test. As may be seen, only the CFM-reinforced composite exhibited any measurable leakage under test conditions.

Tab. 1 Damage extent, residual strength and leakage rate of tested materials

Composite	Damage extent, mm^2		Residual strength, %	Leakage rate, mL/h
	7 J impact	16 J impact		
CFM	460	890	50±29	0,8125
6WR	640	1700	77±19	0
10WR	720	1560	91±14	0
RF	390	1030	67±10	0
TYF	450	990	58±15	0

Fig. 7 presents microsections through the center of the damaged area in the composite materials used in the study. There is a striking difference between CFM-reinforced composite and all of the composites reinforced with woven fabrics. In the latter, the damage consists of delaminations occurring every few plies. In the former, the damage forms conical shape. The centre of this cone is relatively undamaged and seem to be subjected, during the impact event, to translation without deformation. This difference in the character and shape of damage readily explains the lack of leakage through woven-fabric-reinforced composites – through-the-thickness fissures that could allow the water through were present only in mat-reinforced composites.

The question that arises is: why so dramatic difference? Our proposition of the answer stems from the technology of composite manufacture. The continuous-filament mat consists of fibers which are bound with a binding agent, which is soluble in a polyester resin. After the mat is infused, the binding agent dissolves and each lamina disperses, leading to *quasi*-isotropic fiber distribution. In woven fabrics, however, the fiber strands are mechanically bound (woven), so the laminae remain compact and well defined. Between the plies of reinforcement, there exists a layer of neat, non-reinforced resin which constitute ready path for crack transmission.

a)

b)

c)

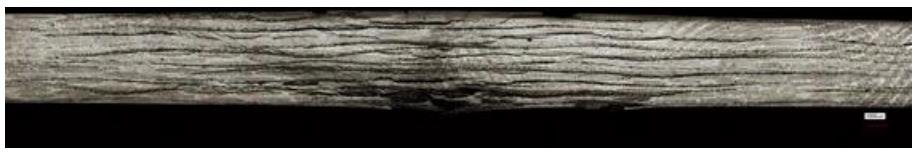

d)

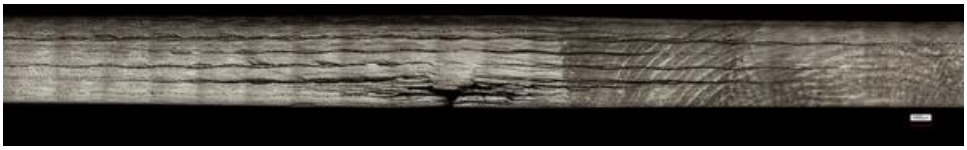

e)

Fig. 7 Microsections through the center of the damaged area in: a) CFM, b) 6RT, c) 10RT, d) RF, and e) TYF after 16 J impact.

4 CONCLUSIONS

- The work demonstrated that the character of damage in composite material depends profoundly on the architecture of the reinforcement.
- The extent of the damage is considerably larger in loose WR-reinforced composites than in either CFM-reinforced ones or composites reinforced with tighter-structured woven fabrics (RF and TYF).
- In multiple-impact test, the increase in damage area after each impact is equal to the area damaged in first impact. CFM-reinforced composites exhibit slower growth of the damaged area then either WR or TYF-reinforced composites. It requires, however, fewer impacts to achieve penetration.
- The residual strength is dependent on reinforcement architecture. The highest was exhibited by woven rovings.
- The damage mode in composites reinforced with mat is strikingly different from that in composites reinforced with woven fabrics, which may be caused by the dissolution of binding agent in the resin. This difference has profound effects for specific applications, such as those requiring leak-resistance.

ACKNOWLEDGEMENT

The work has been supported by the Ministry of Science and Higher Education of the Republic of Poland, grant no. N507 290339.

The work has been performed at the Polymer Institute, West Pomeranian University of Technology, Szczecin as a part of doctoral work.

REFERENCES

[1] AVILA A. F., SOARES M. I., NETO A. S. A study on nanostructured laminated plates behavior under low-velocity impact loading. *International Journal of Impact Engineering*. 2007, XXXIV. Nr. 1, pp. 28-41. ISSN 0734-743X.

[2] SCHRAUWEN B., PEIJS T. Influence of Matrix Ductility and Fibre Architecture on the Repeated Impact Response of Glass-Fibre-Reinforced Laminated Composites. *Applied Composite Materials*. 2002, IX. Nr. 6, pp. 331-352. ISSN 0929-189X.

[3] ABRATE S. *Impact on composite structures*. Cambridge : Cambridge University Press, 1998. 304 pp. ISBN 0521473896.

[4] KUSAKA T., HOJO M., MAI Y.-W., KUROKAWA T., NOJIMA T., OCHIAI S. Rate dependence of mode I fracture behaviour in carbon-fibre/epoxy composite laminates. *Composites Science and Technology*. 1998, LVIII. Nr. 3-4, pp. 591-602. ISSN 0266-3538.

[5] NAIK N. K., SHRIRAO. P. Composite structures under ballistic impact. *Composite Structures*. 2004, LXVI. Nr. 1-4, pp. 579-590. ISSN 0263-8223.

[6] CHEESEMAN B. A., BOGETTI T. A. Ballistic impact into fabric and compliant composite laminates. *Composite Structures*. 2003, LXI. Nr. 1-2, pp. 161-173. ISSN 0263-8223.

[7] OLSSON R. Mass criterion for wave controlled impact response of composite plates. *Composites: Part A*. 2000, XXXI. Nr. 8, pp. 879-887. ISSN 1359-835X.

[8] BLAND P. W., DEAR J. P. Observations on the impact behaviour of carbon-fibre reinforced polymers for the qualitative validation of models. *Composites: Part A*. 2001, XXXII. Nr. 9, pp. 1217-1227. ISSN 1359-835X.

[9] CANTWELL W. J., MORTON J. The impact resistance of composite materials — a review. *Composites*. 1991, XXII. Nr. 5, pp. 347–362. ISSN 0010-4361.

[10] HETHERINGTON J. G. Energy and momentum changes during ballistic perforation. *International Journal of Impact Engineering*. 1996, XVIII. Nr. 3, pp. 319-337. ISSN 0734-743X.

[11] KANG T. J., KIM C. Energy-absorption mechanisms in Kevlar multiaxial warp-knit fabric composites under impact loading. *Composite Science and Technology*. 2000, LX. Nr. 5, pp. 773-784. ISSN 0266-3538.

[12] MORYE S. S., HINE P. J., DUCKET R. A., CARR D. J., WARD I. M. Modelling of the energy absorption by polymer composites upon ballistic impact. *Composite Science and Technology*. 2000, LX. Nr. 14, pp. 2631-2642. ISSN 0266-3538.

[13] NAIK N. K., SHRIRAO P., REDDY B. C. K. Ballistic impact behaviour of woven fabric composites: Formulation. *International Journal of Impact Engineering*. 2006, XXXII. Nr. 9, pp. 1521-1552. ISSN 0734-743X.

[14] REIS L., DE FREITAS M. Damage growth analysis of low velocity impacted composite panels. *Composite Structures*. 1997, XXXVIII. Nr. 1-4, pp. 509-515. ISSN 0263-8223.

[15] HOSUR M. V., KARIM M. R., JEELANI S. Experimental investigation on the response of stitched/unstitched woven S2-glass/SC15 epoxy composites under single and repeated low velocity impact loading. *Composite Structures*. 2003, LXI. Nr. 1-2, pp. 89-102. ISSN 0263-8223.

[16] DA SILVA Jr J. E. L., PACIORNIK S., D'ALMEIDA J. R. M. Determination of the post-ballistic impact mechanical behaviour of a ±45° glass-fabric composite. *Polymer Testing*. 2004, XXIII. Nr. 5, pp. 599-604. ISSN 0142-9418.

[17] PIGGOT M. R. *Load Bearing Fibre Composites*. 2nd ed. Hingham : Kluwer Academic Publishers, 2002. 496 pp. ISBN 079237665X

[18] DELUCA E., PRIFTI J., BETHENEY W., CHOU S. C. Ballistic impact damage of S 2-glass-reinforced plastic structural armour. *Composite Science and Technology*. 1997, LVIII. Nr. 9, pp. 1453-1461. ISSN 0266-3538.

[19] BARCIKOWSKI M. Residual strength of an area of FRP damaged by high-velocity impact. In: *13th Conference Applied Mechanics 2011*. Brno : Ústav fyziky materiálů AV ČR, 2011, pp. 15-18. ISBN 978-80-87434-03-1.

[20] BARCIKOWSKI M., SEMCZYSZYN B. Impact damage in polyester-matrix glass fibre-reinforced composites. Part II. Residual load bearing abilities. *Kompozyty*. 2011, XI. Nr. 3, pp. 235-239. ISSN 2084-6096.

[21] GIBBS & COX *Marine Design Manual For Fiberglass Reinforced Plastics*. New York-Toronto-London : McGraw-Hill Book Company, Inc., 1960. 376 pp. ISBN 0070231753.

[22] KRÓLIKOWSKI W. Einige Eigenschaften der mischverstärkten Polyester-Konstruktionsplatten, besonders bei Zug- und Kugelschlag-Beanspruchung. In *I. Internationale Tagung über Glasfaserverstärkte Kunststoffe und Epoxydharze*, Berlin : Institut für Kunststoffe, 1965, pp. E 4/1-E 4/12.

[23] MOURITZ A. P., GALLAGHER J., GOODWIN A. A. Flexural strength and interlaminar shear strength of stitched GRP laminates following repeated impacts. *Composite Science and Technology*. 1997, LVII. Nr. 5, pp. 509-522. ISSN 0266-3538.

[24] HOSUR M. V., VAIDYA U. K., ULVEN C., JEELANI S. Performance of stitched/unstitched woven carbon/epoxy composites under high velocity impact loading. *Composite Structures*. 2004, LXIV. Nr. 3-4, pp. 455-466. ISSN 0263-8223.

[25] WALKER L., SOHN M. S., HU X.-Z. Improving impact resistance of carbon-fibre composites through interlaminar reinforcement. *Composites: Part A*. 2002, XXXIII. Nr. 6, pp. 893-902. ISSN 1359-835X.

[26] GU B., XU J. Finite element calculation of 4-step 3-dimensional braided composite under ballistic perforation. *Composites: Part B*. 2004, XXXV. Nr. 4, pp. 291-297. ISSN 1359-8368.